ACS APPLIED MATERIALS & INTERFACES

Letter

Cite This: ACS Appl. Mater. Interfaces 2018, 10, 10601−10606

www.acsami.org

Glutathione-Depleting Gold Nanoclusters for Enhanced Cancer Radiotherapy through Synergistic External and Internal Regulations

Xiaodong Zhang,[†] Xiaokai Chen,[†] Yao-Wen Jiang,[†] Ningning Ma,[†] Liu-Yuan Xia,[†] Xiaotong Cheng,[†] Hao-Ran Jia,[†] Peidang Liu,[‡] Ning Gu,[†] Zhan Chen,*[,§] and Fu-Gen Wu*[,†]

[†]State Key Laboratory of Bioelectronics, School of Biological Science and Medical Engineering, Southeast University, Nanjing 210096, China

[‡]School of Medicine, Southeast University, Nanjing 210009, China

[§]Department of Chemistry, University of Michigan, 930 North University Avenue, Ann Arbor, Michigan 48109, United States

Supporting Information

ABSTRACT: The therapeutic performance of cancer radiotherapy is often limited by the overexpression of glutathione (GSH) in tumors and low radiation sensitivity of cancerous cells. To address these issues, the facilely prepared histidine-capped gold nanoclusters (Au NCs@His) were adopted as a radiosensitizer with a high sensitization enhancement ratio of ∼1.54. On one hand, Au NCs@His can inherit the local radiation enhancement property of gold-based materials (external regulation); on the other hand, Au NCs@His can decrease the intracellular GSH level, thus preventing the generated reactive oxygen species (ROS) from being consumed by GSH, and arrest the cells at the radiosensitive G2/M phase (internal regulation).

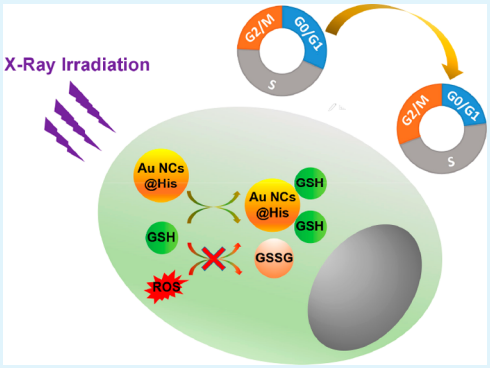

KEYWORDS: *gold nanoclusters, radiotherapy, radiosensitizer, GSH depletion, regulation of the cell cycle*

Radiotherapy, one of the mainstream cancer treatment methods, utilizes ionizing radiation to kill cancer cells.[1,2] Nevertheless, owing to the low radiation absorbability of the tumor tissue,[2] high energy radiation is employed during the treatment, leading to undesirable damage to normal tissues.[1] To address this issue, radiosensitizers are applied to increase the local treatment efficiency under a relatively low radiation dose.[3]

In recent years, nanoradiosensitizers have been widely studied due to their better tumor-targeting ability and higher cellular internalization compared with traditional molecular radiosensitizers. These nanoradiosensitizers usually contain high-*Z* elements such as bismuth (83),[4,5] gold (79),[6−9] tungsten (74),[10,11] tantalum (73),[12] and hafnium (72),[13] which can increase the local radiation dose through absorbing, scattering, and emitting radiation energy.[3] Besides, some high-*Z* element-free nanomaterials, such as silver nanoparticles[14] and iron oxide nanoparticles,[15] can also be radiosensitizers through releasing Ag^+ or Fe^{3+} to promote intracellular reactive oxygen species (ROS) production.[2] However, most of these materials are still not ideal for radiotherapy. Two possible reasons may be responsible for their weak radiosensitizing effect: (1) Some cancer cells, especially tumor stem cells, have inherent radiation-tolerance ability.[16] (2) The high concentration of glutathione (GSH, an antioxidant) in the tumor cells can consume the ROS, thus decreasing the ROS level for protecting the tumor cells.[17−19]

On the other hand, gold nanoclusters (Au NCs) are a class of zero-dimensional nanomaterials with a typical diameter of <5 nm.[20] Owning to their unique physicochemical properties and excellent biocompatibility, Au NCs can be used for catalysis,[21] molecular/ion detection,[22,23] and potential biological applications.[24−27] In a previous study, we demonstrated that histidine-capped Au NCs (Au NCs@His) prepared by blending histidine and $HAuCl_4$ could bind tightly and selectively with GSH through a Au−S bond.[28] Besides, it has been reported that gold-based materials can cause the cell cycle accumulation in the G2/M phase,[29] which is considered to be a radiation-sensitive phase. Inspired by these, we hypothesize that Au NCs@His can be an effective radiosensitizer through synergistic external and internal regulations (Scheme 1): On one hand, Au NCs@His can inherit the local radiation enhancement property of gold-based materials (external regulation); on the other hand, Au NCs@His can reverse the radiation tolerance of cancer cells through decreasing the intracellular level of GSH and regulating the cell cycle to the radiation-sensitive phase (internal regulation).

Au NCs@His were prepared simply by mixing $HAuCl_4$ aqueous solution (1 mL, 10 mM) and histidine solution (3 mL, 100 mM), followed by further incubation at ambient

Received: January 5, 2018
Accepted: March 15, 2018
Published: March 15, 2018

DOI: 10.1021/acsami.8b00207
ACS Appl. Mater. Interfaces 2018, 10, 10601−10606

Scheme 1. Schematic Illustration of the Therapeutic Principle Based on Au NCs@His for Simultaneously Increasing ROS Generation, Depleting Glutathione, and Regulating Cell Cycle

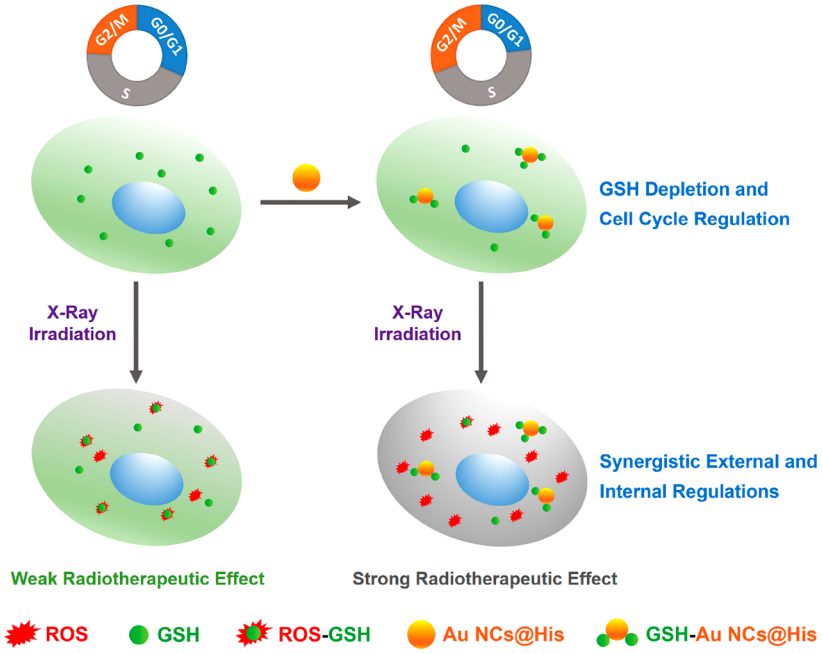

temperature without stirring for 4 h.[28] They were stable for more than 14 days at 4 °C in various solutions including water, phosphate-buffered saline (PBS), fetal bovine serum, and Dulbecco's modified Eagle's medium (DMEM) (Figure S1). The facile preparation and excellent aqueous stability ensure the further applications of the as-prepared Au NCs@His. To verify that the GSH depletion property is a main reason for Au NCs@His to enhance the radiosensitizing effect, Au NCs@His preincubated with GSH (GSH-Au NCs@His) were prepared by mixing Au NCs@His solution and GSH solution with the GSH/Au molar ratio of 12:1. According to the TEM images, the two types of Au NCs have a similar size distribution with a diameter of ∼3 nm (Figure 1a and 1b). After adding GSH to Au NCs@His, the changes in hydrodynamic diameter (from 4.0 to 6.3 nm, Figure 1c), zeta potential (from −15.8 to −6.4 mV, Figure 1d), UV−vis absorption peak (from ∼334 to ∼415 nm, Figure 1e), and fluorescence intensity (∼20-fold increase, Figure 1f) all confirmed the successful synthesis of GSH-Au NCs@His. The enhanced fluorescence intensity of GSH-Au NCs@His as compared to that of Au NCs@His can be explained by the following reasons: One is the "charge transfer from the ligands to the metal center (LMNCT)" mechanism.[28] Charge transfer might occur between Au NCs@His and GSH through the Au−S bond. Meanwhile, GSH contains many electron-rich carboxyl and amine groups, which might also contribute to the fluorescence enhancement. Besides, the changed structure after adding GSH is another possible explanation,[25] which can enhance the coordination stability to metal atoms.

In the following research, we used both Au NCs@His and GSH-Au NCs@His in all the experiments and found that Au NCs@His exhibited a better radiosensitization effect as compared to GSH-Au NCs@His.

To study the cytotoxicity of Au NCs@His and GSH-Au NCs@His, murine cervical carcinoma U14 cells were selected (Figure 1g). MTT results show that Au NCs@His were more toxic to the cells than GSH-Au NCs@His, which is in accordance with our previous results.[28] The high toxicity of Au NCs@His may be attributed to their GSH depletion property, which prevents ROS from being consumed by GSH. Nevertheless, when the Au concentration decreased to 100 μM or below, both Au NCs@His and GSH-Au NCs@His had low toxicity to the cells. Thus, 100 μM was selected as the working concentration in the following experiments.

It is known that a high cellular internalization of Au-based nanomaterials has a positive effect on the radiosensitizing effect.[30] In view of this, the endocytosed amounts of the two Au NCs were compared. The contents of the cells and Au were determined by flow cytometry and inductively coupled plasma optical emission spectrometry (ICP-OES), respectively. Figure 1h shows that Au NCs@His- and GSH-Au NCs@His-treated cells had similar endocytosed Au content per cell with a concentration of ∼1.8 ng/cell. To further visualize the intracellular distribution of Au NCs@His and GSH-Au NCs@His, confocal imaging experiments were conducted (Figure 1i). After the addition of Au NCs@His, some bright cyan fluorescent dots were formed within the cells, which were as bright as those within the GSH-Au NCs@His-treated cells. The results likely indicate the binding between Au NCs@His and the intracellular GSH. Besides, the GSH levels without and with Au NCs@His treatment were determined using a total GSH detection kit. The results showed that the total GSH content was similar in the two groups, while the unbound GSH level in the Au NCs@His-treated cells drastically decreased from 1.86 to 0.42 mM compared with that in the control group (Figure S2), further demonstrating the glutathione-depleting ability of Au NCs@His.

To evaluate the sensitization efficiency of Au NCs@His and GSH-Au NCs@His, colony formation experiments were carried out using U14 cells. It was observed that both of the Au NCs could enhance the radiotherapeutic efficiency at all the tested radiation doses (Figure 2a and S3). Using the classical multitarget single-hit model, the sensitization enhancement ratio (SER) of Au NCs@His was calculated to be 1.54, which

DOI: 10.1021/acsami.8b00207
ACS Appl. Mater. Interfaces 2018, 10, 10601−10606

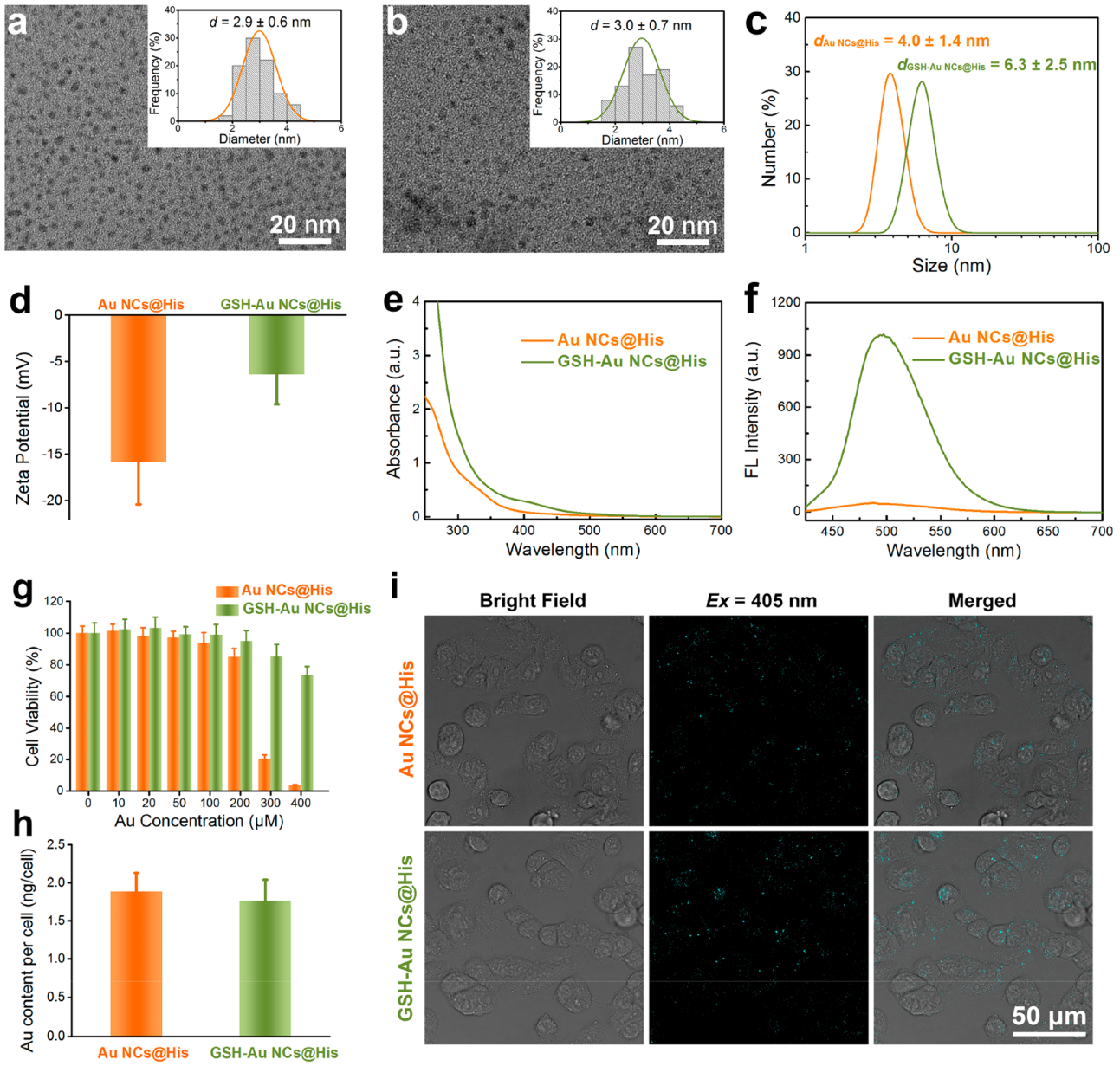

Figure 1. (a and b) Typical TEM images and the corresponding size distribution histograms of Au NCs@His and GSH-Au NCs@His, respectively. (c) Dynamic light scattering and (d) zeta potential results of Au NCs@His and GSH-Au NCs@His. (e) UV−vis and (f) FL spectra of Au NCs@His and GSH-Au NCs@His. (g) Cell viability of U14 cells treated with various concentrations of Au NCs@His or GSH-Au NCs@His. (h) Au content per cell after incubation with Au NCs@His or GSH-Au NCs@His (Au concentration: 100 μM) for 24 h. (i) Confocal images of U14 cells after incubation with Au NCs@His or GSH-Au NCs@His (Au concentration: 100 μM) for 24 h.

was higher than those of GSH-Au NCs@His (~1.25) and most of the other nanoradiosensitizers (Table S1). To further demonstrate the strong radiosensitizing effect of Au NCs@His, immunofluorescence assay for phosphorylated Ser 139 on histone H2AX (γ-H2AX) was carried out to evaluate the DNA damage level (Figure 2b and 2c). It can be seen that the DNA damage levels of all the groups significantly increased after the X-ray irradiation treatment. Specifically, the mean number of γ-H2AX in the Au NCs@His-treated cells was nearly twice as high as that in the control group after the X-ray irradiation treatment. In contrast, GSH-Au NCs@His could only slightly increase the DNA damage level (~1.3-fold) as compared to the control group.

To reveal the possible mechanism of the strong radiosensitizing effect of Au NCs@His, the intracellular ROS level was evaluated using flow cytometry. Figure 2d and 2e show that after X-ray irradiation the ROS levels in Au NCs@His- and GSH-Au NCs@His-treated cells were higher than those in the corresponding control groups, indicating that the two Au NCs can promote the ROS generation under irradiation treatment. Besides, the ROS enhancement ability of Au NCs@His was stronger than that of GSH-Au NCs@His, suggesting that Au NCs@His can be a GSH scavenger to protect the generated ROS from being consumed.

Next, we would like to investigate the effect of the change in cell cycle distribution on the radiosensitizing performance of the two types of Au NCs using flow cytometry combined with propidium iodide (PI) staining (Figure 2f). It can be seen that without Au NCs the percentage of the G2/M phase of the cells significantly decreased after the treatment with X-ray

DOI: 10.1021/acsami.8b00207
ACS Appl. Mater. Interfaces 2018, 10, 10601−10606

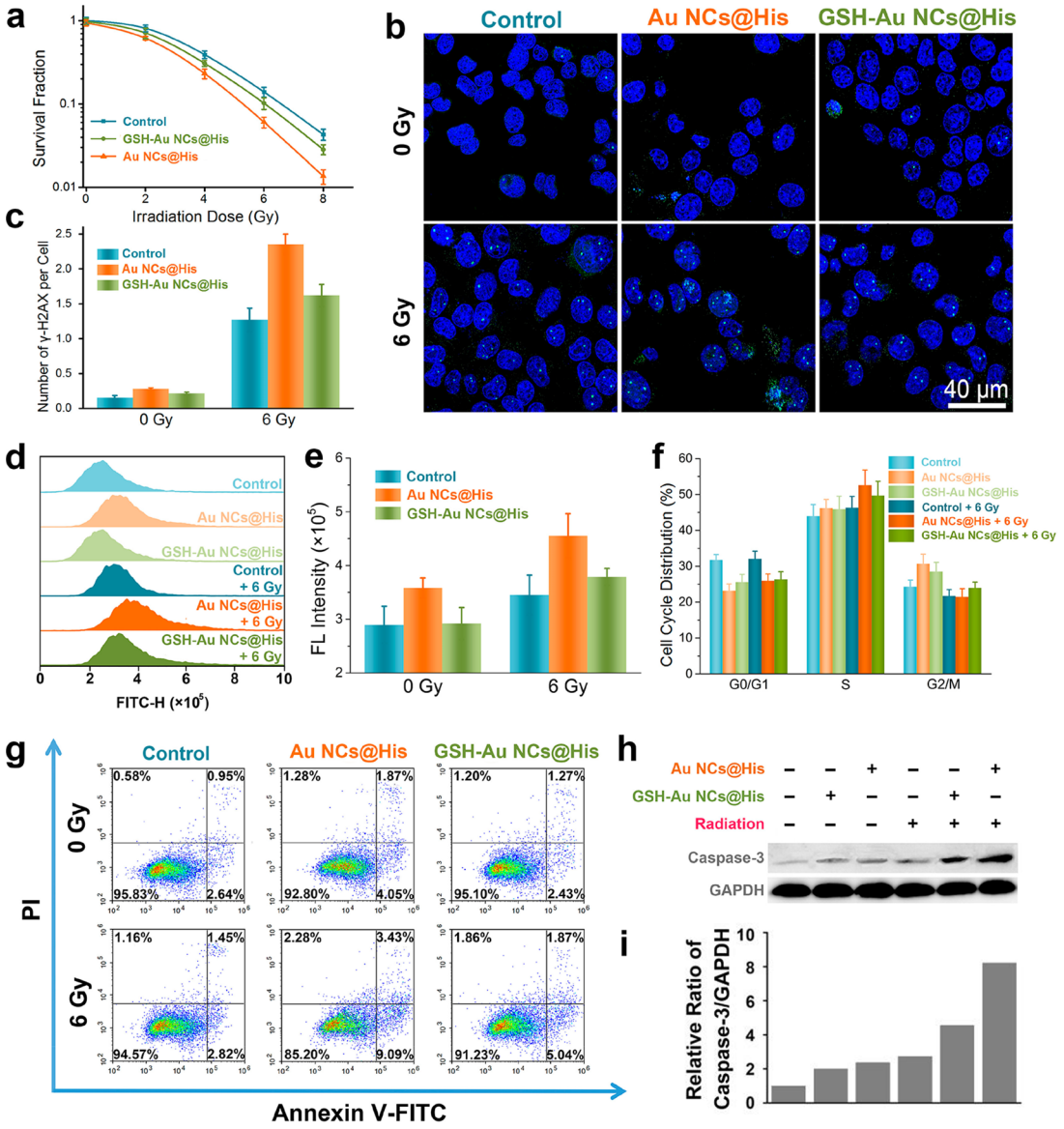

Figure 2. (a) Survival fractions of U14 cells after treatment with Au NCs@His or GSH-Au NCs@His (Au concentration: 100 μM). (b) Confocal fluorescence images of γ-H2AX and (c) the corresponding statistical result of γ-H2AX per cell (counted manually) induced by different treatments as indicated (Au concentration: 100 μM). The cells were stained with Alexa Fluor 488-conjugated γ-H2AX monoclonal antibody (green) and Hoechst 33342 (blue) for visualizing DNA fragmentation and nucleus, respectively. (d) ROS generation level of U14 cells after various treatments and (e) the corresponding statistical results. (f) Cell cycle distribution of U14 cells after various treatments. (g) Apoptosis results of U14 cells after various treatments. (h) Image and (i) the corresponding statistical histogram of Western blotting results. GAPDH serves as a loading control.

irradiation, indicating that the cells in the G2/M phase are more radiosensitive than those in other phases. Meanwhile, the treatment with Au NCs@His or GSH-Au NCs@His could induce the acceleration of the G0/G1 phase and accumulation of cells in the G2/M phase, which is consistent with the effects of other gold-based nanomaterials.[29] The cell cycle distribution results indicate that Au NCs could promote more cells to be arrested at the radiosensitive G2/M phase, which is beneficial for achieving better radiotherapeutic outcomes.

The radiation sensitization effect of Au NCs@His was further studied by apoptosis assay (Figure 2g). The apoptosis ratio of the cells slightly increased from 3.59% to 4.27% after the irradiation treatment alone. The combined treatment with GSH-Au NCs@His and X-ray irradiation could increase the apoptosis ratio from 3.70% to 6.91%. In contrast, a sharp increase of apoptosis ratio (from 5.92% to 12.52%) was observed when the cells were treated with both Au NCs@His and X-ray irradiation. To further compare the apoptosis level of cells after various treatments, the expression of active caspase-3, an apoptosis marker protein, was determined using Western blotting assay (Figure 2h and 2i). Similarly, the combined treatment with Au NCs@His and X-ray irradiation could remarkably up-regulate the expression of active caspase-3 compared to the treatment with X-ray irradiation alone and the combined treatment with GSH-Au NCs@His and X-ray irradiation. The above results indicate that the increase in the apoptosis level is the possible mechanism by which Au NCs@His induced a higher level of cell death after X-ray irradiation.

Finally, the *in vivo* therapeutic effect and safety of Au NCs@His were evaluated (Figure 3). The mice were intratumorally injected with Au NCs@His or GSH-Au NCs@His and exposed to radiation after 4 h postinjection (p.i.). As shown in Figure 3a,

DOI: 10.1021/acsami.8b00207
ACS Appl. Mater. Interfaces 2018, 10, 10601−10606

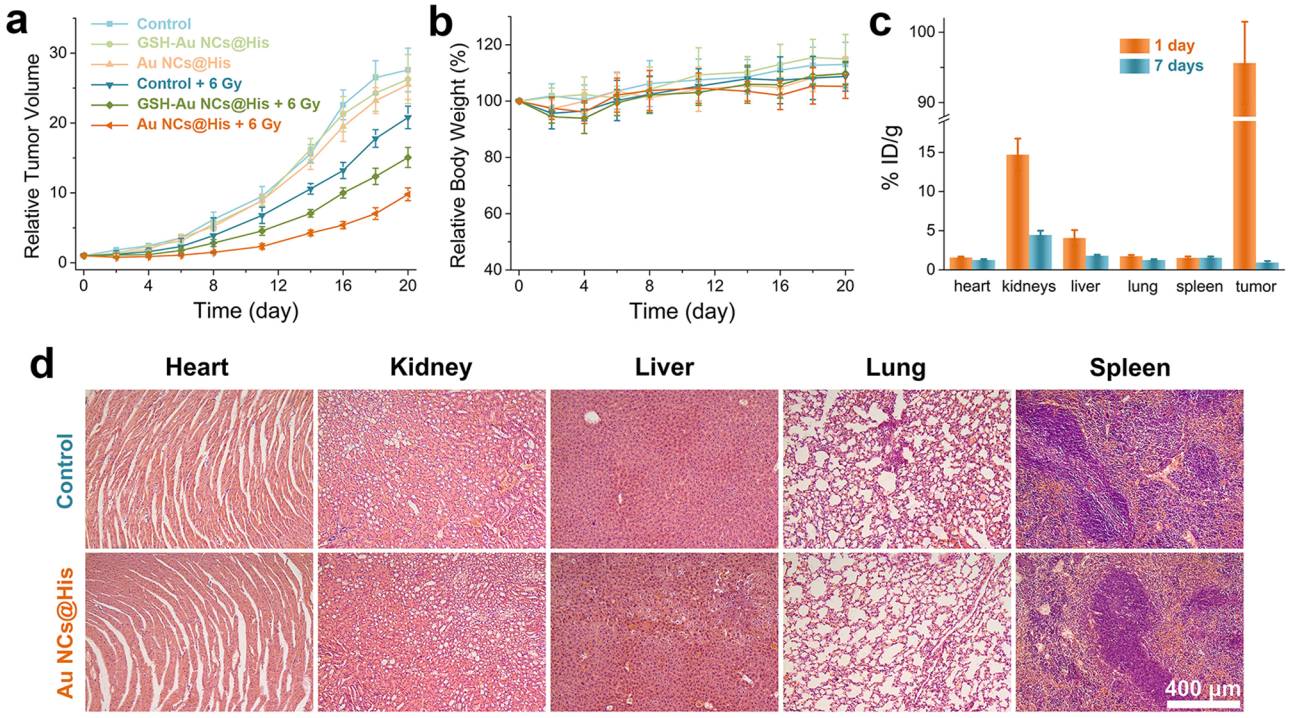

Figure 3. (a) Relative tumor growth and (b) body weight curves of mice after various treatments. (c) Biodistribution of Au NCs@His at 1 day and 7 days after intratumoral injection. (d) Histological evaluation of different organs (including heart, liver, spleen, lung, and kidneys) from mice after treatment with PBS (control) or Au NCs@His for 20 days.

the relative tumor growth curves of the groups without radiotherapy have a similar trend, indicating that the two Au NCs had negligible effect on the tumor growth. The tumors in mice receiving only X-ray irradiation regrew in 2 days. In contrast, the combination treatment of Au NCs@His and X-ray irradiation could inhibit the tumor growth for ~6 days, and such a combined treatment exhibited the best tumor growth inhibition effect as compared to other groups. These results further confirm the excellent radiosensitizing effect of Au NCs@His. Besides, the body weights of mice throughout the experimental period were monitored (Figure 3b). No evident body weight loss was observed in Au NCs@His-treated groups, suggesting the little toxicity of the nanoagents. We have also studied the biodistribution and body clearance of Au NCs@His at 1 day and 7 days p.i. (Figure 3c). At 1 day p.i., tumor and kidneys were the two main distribution organs (~95.6% ID/g in tumor and 14.7% ID/g in kidneys), indicating that Au NCs@His have long-term tumor retention and can be excreted through kidneys. The Au content in the tumor decreased to ~0.94% ID/g at 7 days p.i., suggesting that the renal clearance of Au NCs@His was quite effective. Systemic toxicity was further evaluated by analyzing the tissue slices from mice administered with Au NCs@His for 20 days (Figure 3d). No obvious inflammation, cell necrosis, or apoptosis was observed in the main organs including heart, liver, spleen, lung, and kidneys, indicating the excellent biocompatibility of Au NCs@His.

In this work, we report for the first time that the facilely prepared Au NCs@His exhibit strong radiosensitizing effect through simultaneous external and internal regulations. Besides inheriting the radiosensitizing property of gold-based nanomaterials, Au NCs@His can also deplete the intracellular antioxidants (e.g., GSH) and regulate the cell cycle to accumulate in the radiosensitizing G2/M phase. As a result, the SER of Au NCs@His was calculated to be 1.54, which is higher than those of most metal-based radiosensitizers. Moreover, *in vivo* experiments showed the good tumor inhibition ability and fast renal clearance of Au NCs@His. It is hoped that the GSH-depleting strategy developed in this work can provide a new strategy for designing radiosensitizers and will find potential applications in cancer radiotherapy.

■ ASSOCIATED CONTENT

Supporting Information

The Supporting Information is available free of charge on the ACS Publications website at DOI: 10.1021/acsami.8b00207.

Experimental details, photographs of Au NCs@His solutions, GSH content histogram, colony formation images, and SER table (PDF)

■ AUTHOR INFORMATION

Corresponding Authors

*E-mail: wufg@seu.edu.cn.
*E-mail: zhanc@umich.edu.

ORCID

Xiaodong Zhang: 0000-0003-4137-3535
Ning Gu: 0000-0003-0047-337X
Zhan Chen: 0000-0001-8687-8348
Fu-Gen Wu: 0000-0003-1773-2868

Notes

The authors declare no competing financial interest.

■ ACKNOWLEDGMENTS

This work was supported by National Natural Science Foundation of China (21673037 and 81571805), Natural Science Foundation of Jiangsu Province (BK20170078),

DOI: 10.1021/acsami.8b00207
ACS Appl. Mater. Interfaces 2018, 10, 10601−10606

Innovative and Entrepreneurial Talent Recruitment Program of Jiangsu Province, Six Talents Peak Project in Jiangsu Province (2015-SWYY-003), the Fundamental Research Funds for the Central Universities, Postgraduate Research&Practice Innovation Program of Jiangsu Province (KYCX17_0155 and KYCX17_0157), the Scientific Research Foundation of Graduate School of Southeast University (YBJJ1777 and YBJJ1778), and the Scientific Research Foundation for Returned Overseas Chinese Scholars, State Education Ministry. Z.C. thanks the University of Michigan for the support.

REFERENCES

(1) Jaffray, D. A. Image-Guided Radiotherapy: from Current Concept to Future Perspectives. *Nat. Rev. Clin. Oncol.* **2012**, *9*, 688−699.
(2) Song, G. S.; Cheng, L.; Chao, Y.; Yang, K.; Liu, Z. Emerging Nanotechnology and Advanced Materials for Cancer Radiation Therapy. *Adv. Mater.* **2017**, *29*, 1700996.
(3) Goswami, N.; Luo, Z. T.; Yuan, X.; Leong, D. T.; Xie, J. P. Engineering Gold-Based Radiosensitizers for Cancer Radiotherapy. *Mater. Horiz.* **2017**, *4*, 817−831.
(4) Wang, Y.; Wu, Y. Y.; Liu, Y. J.; Shen, J.; Lv, L.; Li, L. B.; Yang, L. C.; Zeng, J. F.; Wang, Y. Y.; Zhang, L. W.; Li, Z.; Gao, M. Y.; Chai, Z. F. BSA-Mediated Synthesis of Bismuth Sulfide Nanotheranostic Agents for Tumor Multimodal Imaging and Thermoradiotherapy. *Adv. Funct. Mater.* **2016**, *26*, 5335−5344.
(5) Guo, Z.; Zhu, S.; Yong, Y.; Zhang, X.; Dong, X. H.; Du, J. F.; Xie, J. N.; Wang, Q.; Gu, Z. J.; Zhao, Y. L. Synthesis of BSA-Coated BiOI@Bi_2S_3 Semiconductor Heterojunction Nanoparticles and Their Applications for Radio/Photodynamic/Photothermal Synergistic Therapy of Tumor. *Adv. Mater.* **2017**, *29*, 1704136.
(6) Zhang, X. D.; Wu, D.; Shen, X.; Chen, J.; Sun, Y. M.; Liu, P. X.; Liang, X. J. Size-Dependent Radiosensitization of PEG-Coated Gold Nanoparticles for Cancer Radiation Therapy. *Biomaterials* **2012**, *33*, 6408−6419.
(7) Zhang, X. D.; Luo, Z. T.; Chen, J.; Shen, X.; Song, S. S.; Sun, Y. M.; Fan, S. J.; Fan, F. Y.; Leong, D. T.; Xie, J. P. Ultrasmall $Au_{(10-12)}(SG)_{(10-12)}$ Nanomolecules for High Tumor Specificity and Cancer Radiotherapy. *Adv. Mater.* **2014**, *26*, 4565−4568.
(8) Ma, N. N.; Jiang, Y. W.; Zhang, X. D.; Wu, H.; Myers, J. N.; Liu, P. D.; Jin, H. Z.; Gu, N.; He, N. Y.; Wu, F. G.; Chen, Z. Enhanced Radiosensitization of Gold Nanospikes via Hyperthermia in Combined Cancer Radiation and Photothermal Therapy. *ACS Appl. Mater. Interfaces* **2016**, *8*, 28480−28494.
(9) Liu, X.; Zhang, X.; Zhu, M.; Lin, G. H.; Liu, J.; Zhou, Z. F.; Tian, X.; Pan, Y. PEGylated Au@Pt Nanodendrites as Novel Theranostic Agents for Computed Tomography Imaging and Photothermal/Radiation Synergistic Therapy. *ACS Appl. Mater. Interfaces* **2017**, *9*, 279−285.
(10) Yong, Y.; Cheng, X. J.; Bao, T.; Zu, M.; Yan, L.; Yin, W. Y.; Ge, C. C.; Wang, D. L.; Gu, Z. J.; Zhao, Y. L. Tungsten Sulfide Quantum Dots as Multifunctional Nanotheranostics for in Vivo Dual-Modal Image-Guided Photothermal/Radiotherapy Synergistic Therapy. *ACS Nano* **2015**, *9*, 12451−12463.
(11) Wen, L.; Chen, L.; Zheng, S. M.; Zeng, J. F.; Duan, G. X.; Wang, Y.; Wang, G. L.; Chai, Z. F.; Li, Z.; Gao, M. Y. Ultrasmall Biocompatible WO_{3-x} Nanodots for Multi-Modality Imaging and Combined Therapy of Cancers. *Adv. Mater.* **2016**, *28*, 5072−5079.
(12) Song, G. S.; Chao, Y.; Chen, Y. Y.; Liang, C.; Yi, X.; Yang, G. B.; Yang, K.; Cheng, L.; Zhang, Q.; Liu, Z. All-in-One Theranostic Nanoplatform Based on Hollow TaOx for Chelator-Free Labeling Imaging, Drug Delivery, and Synergistically Enhanced Radiotherapy. *Adv. Funct. Mater.* **2016**, *26*, 8243−8254.
(13) Liu, J. J.; Yang, Y.; Zhu, W. W.; Yi, X.; Dong, Z. L.; Xu, X. N.; Chen, M. W.; Yang, K.; Lu, G.; Jiang, L. X.; Liu, Z. Nanoscale Metal-Organic Frameworks for Combined Photodynamic & Radiation Therapy in Cancer Treatment. *Biomaterials* **2016**, *97*, 1−9.
(14) Wu, H.; Lin, J.; Liu, P. D.; Huang, Z. H.; Zhao, P.; Jin, H. Z.; Wang, C. L.; Wen, L. P.; Gu, N. Is the Autophagy a Friend or Foe in the Silver Nanoparticles Associated Radiotherapy for Glioma? *Biomaterials* **2015**, *62*, 47−57.
(15) Hauser, A. K.; Mitov, M. I.; Daley, E. F.; McGarry, R. C.; Anderson, K. W.; Hilt, J. Z. Targeted Iron Oxide Nanoparticles for the Enhancement of Radiation Therapy. *Biomaterials* **2016**, *105*, 127−135.
(16) Rich, J. N. Cancer Stem Cells in Radiation Resistance. *Cancer Res.* **2007**, *67*, 8980−8984.
(17) Biaglow, J. E.; Varnes, M. E.; Epp, E. R.; Clark, E. P.; Astor, M. Factors Involved on Depletion of Glutathione from A549 Human Lung Carcinoma Cells: Implications for Radiotherapy. *Int. J. Radiat. Oncol., Biol., Phys.* **1984**, *10*, 1221−1227.
(18) Fan, H. H.; Yan, G. B.; Zhao, Z. L.; Hu, X. X.; Zhang, W. H.; Liu, H.; Fu, X. Y.; Fu, T.; Zhang, X. B.; Tan, W. H. A Smart Photosensitizer-Manganese Dioxide Nanosystem for Enhanced Photodynamic Therapy by Reducing Glutathione Levels in Cancer Cells. *Angew. Chem., Int. Ed.* **2016**, *55*, 5477−5482.
(19) Ju, E. G.; Dong, K.; Chen, Z. W.; Liu, Z.; Liu, C. Q.; Huang, Y. Y.; Wang, Z. Z.; Pu, F.; Ren, J. S.; Qu, X. G. Copper(II)-Graphitic Carbon Nitride Triggered Synergy: Improved ROS Generation and Reduced Glutathione Levels for Enhanced Photodynamic Therapy. *Angew. Chem., Int. Ed.* **2016**, *55*, 11467−11471.
(20) Tao, Y.; Li, M. Q.; Ren, J. S.; Qu, X. G. Metal Nanoclusters: Novel Probes for Diagnostic and Therapeutic Applications. *Chem. Soc. Rev.* **2015**, *44*, 8636−8663.
(21) Zhao, S.; Jin, R. X.; Abroshan, H.; Zeng, C. J.; Zhang, H.; House, S. D.; Gottlieb, E.; Kim, H. J.; Yang, J. C.; Jin, R. C. Gold Nanoclusters Promote Electrocatalytic Water Oxidation at the Nanocluster/$CoSe_2$ Interface. *J. Am. Chem. Soc.* **2017**, *139*, 1077−1080.
(22) Huang, C. C.; Yang, Z.; Lee, K. H.; Chang, H. T. Synthesis of Highly Fluorescent Gold Nanoparticles for Sensing Mercury(II). *Angew. Chem., Int. Ed.* **2007**, *46*, 6824−6828.
(23) Sun, S. S.; Ning, X. H.; Zhang, G.; Wang, Y. C.; Peng, C. Q.; Zheng, J. Dimerization of Organic Dyes on Luminescent Gold Nanoparticles for Ratiometric pH Sensing. *Angew. Chem., Int. Ed.* **2016**, *55*, 2421−2424.
(24) Shang, L.; Stockmar, F.; Azadfar, N.; Nienhaus, G. U. Intracellular Thermometry by Using Fluorescent Gold Nanoclusters. *Angew. Chem., Int. Ed.* **2013**, *52*, 11154−11157.
(25) Chen, L. Y.; Wang, C. W.; Yuan, Z. Q.; Chang, H. T. Fluorescent Gold Nanoclusters: Recent Advances in Sensing and Imaging. *Anal. Chem.* **2015**, *87*, 216−229.
(26) Zhang, X. D.; Wu, F. G.; Liu, P. D.; Wang, H. Y.; Gu, N.; Chen, Z. Synthesis of Ultrastable and Multifunctional Gold Nanoclusters with Enhanced Fluorescence and Potential Anticancer Drug Delivery Application. *J. Colloid Interface Sci.* **2015**, *455*, 6−15.
(27) Zhang, W. S.; Lin, D. M.; Wang, H. X.; Li, J. F.; Nienhaus, G. U.; Su, Z. Q.; Wei, G.; Shang, L. Supramolecular Self-Assembly Bioinspired Synthesis of Luminescent Gold Nanocluster-Embedded Peptide Nanofibers for Temperature Sensing and Cellular Imaging. *Bioconjugate Chem.* **2017**, *28*, 2224−2229.
(28) Zhang, X. D.; Wu, F. G.; Liu, P. D.; Gu, N.; Chen, Z. Enhanced Fluorescence of Gold Nanoclusters Composed of $HAuCl_4$ and Histidine by Glutathione: Glutathione Detection and Selective Cancer Cell Imaging. *Small* **2014**, *10*, 5170−5177.
(29) Roa, W.; Zhang, X. J.; Guo, L. H.; Shaw, A.; Hu, X. Y.; Xiong, Y. P.; Gulavita, S.; Patel, S.; Sun, X. J.; Chen, J.; Moore, R.; Xing, J. Z. Gold Nanoparticle Sensitize Radiotherapy of Prostate Cancer Cells by Regulation of the Cell Cycle. *Nanotechnology* **2009**, *20*, 375101.
(30) Ma, N. N.; Wu, F. G.; Zhang, X. D.; Jiang, Y. W.; Jia, H. R.; Wang, H. Y.; Li, Y. H.; Liu, P. D.; Gu, N.; Chen, Z. Shape-Dependent Radiosensitization Effect of Gold Nanostructures in Cancer Radiotherapy: Comparison of Gold Nanoparticles, Nanospikes, and Nanorods. *ACS Appl. Mater. Interfaces* **2017**, *9*, 13037−13048.

DOI: 10.1021/acsami.8b00207
ACS Appl. Mater. Interfaces 2018, 10, 10601−10606